Available online at www.sciencedirect.com
ScienceDirect
Journal of Catalysis 250 (2007) 139–150
JOURNAL OF CATALYSIS
www.elsevier.com/locate/jcat

Deactivation of a Au/CeO_2 catalyst during the low-temperature water–gas shift reaction and its reactivation: A combined TEM, XRD, XPS, DRIFTS, and activity study

A. Karpenko [a], R. Leppelt [a], J. Cai [a], V. Plzak [b], A. Chuvilin [c], U. Kaiser [c], R.J. Behm [a,*]

[a] *Institute of Surface Chemistry and Catalysis, Ulm University, D-89069 Ulm, Germany*
[b] *Centre for Solar Energy and Hydrogen Research, Helmholtzstr. 8, D-89081 Ulm, Germany*
[c] *Centre of Electron Microscopy, Ulm University, D-89069 Ulm, Germany*

Received 29 March 2007; revised 18 May 2007; accepted 21 May 2007

Available online 10 July 2007

Abstract

The deactivation of Au/CeO_2 catalysts during low-temperature water–gas shift reaction and the underlying physical origin were investigated, comparing the deactivation in different reaction atmospheres and subsequent regeneration of the catalysts by reactive treatment in O_2/N_2 or H_2O/N_2 gas mixtures. Based on TEM and XRD measurements, Au and ceria particle sintering (irreversible deactivation) can be excluded as reasons for the deactivation. In addition to the formation of adsorbed monodentate carbonate species, which we recently identified as a major reason for catalyst deactivation under present reaction conditions [Denkwitz et al., J. Catal. 246 (2007) 74], XPS measurements show significant variations in Ce^{3+} and Au^{n+} content during reaction in different atmospheres and on regeneration. Reaction generally leads to increasing catalyst reduction (i.e., decreased Au^{n+} content and increased Ce^{3+} content); this is reversed during regeneration. The correlation between the relative content of these ionic species and the catalytic activity is not as clear as that between carbonate formation/decomposition and deactivation/regeneration, leaving monodentate carbonate formation as the dominant but not sole reason for catalyst deactivation.

Keywords: Water–gas shift reaction; Au/CeO_2 catalyst; Deactivation; Reactivation; GC; DRIFTS; XPS; TEM; XRD

1. Introduction

Au/CeO_2 catalysts have been reported to be highly active for catalyzing the water–gas shift reaction at low temperatures, which makes them interesting candidates for applications in which low temperatures are or may be beneficial, such as feed gas cleanup for low-temperature fuel cells [1–24]. But the technical application of these catalysts is hindered by their tendency for deactivation under these reaction conditions. The physical origin and mechanism of the deactivation process are controversial, and different explanations have been put forward to explain this in a molecular picture, including sintering of the metal particles [9], loss of ceria surface area [6], overreduction of the ceria support (for Pt/CeO_2 catalysts) [25], and increased blocking of the ceria surface by formation of surface carbonates, formats, or hydroxycarbonates [17,18,24,26]. On the other hand, another long-term study found no deactivation [7]. A coherent picture remains elusive. The varying results and conclusions from these studies can be explained at least partly by the rather different morphologies and surface compositions of the catalysts, due to differing procedures for catalyst pretreatment and differing reaction conditions. Furthermore, deactivation may be caused by different effects simultaneously, such as Au particle sintering and catalyst reduction, that are either independent of each other or correlated. In most studies, however, attention was paid to one or two different possible effects, leaving open the possibility that other effects besides those proposed might contribute to the deactivation. Third, a consistent picture of deactivation would require an at least semiquantitative correlation between the change in (surface) properties of the catalyst and the loss of catalytic activity during reaction under different reaction con-

* Corresponding author.
E-mail address: juergen.behm@uni-ulm.de (R.J. Behm).

0021-9517/$ – see front matter
doi:10.1016/j.jcat.2007.05.016

ditions. Such comprehensive information on the deactivation behavior has not been reported so far.

Earlier, we had demonstrated, by simultaneously following the deactivation of the catalyst and the buildup of adsorbed species via in situ diffuse reflectance Fourier transform IR (DRIFTS) measurements in different reaction atmospheres, that under typical reaction conditions (180 °C), the deactivation is essentially quantitatively correlated with the buildup of stable monodentate surface carbonate species on the ceria support [24]. But possible contributions from other mechanisms were not tested and thus could not be ruled out in that study. This is the topic of the present study, where we investigated the reaction-induced effects on the size of the Au and ceria particles and on the surface composition of the same catalyst and under identical reaction conditions as previous work [24]. We evaluated particle sizes before and after 1000 min of reaction by transmission electron microscopy (TEM) and X-ray diffraction (XRD) measurements, and investigated the surface composition by X-ray photoemission spectroscopy (XPS). Furthermore, we studied the effect of a sudden decrease in reaction temperature, as experienced on, for example, a shutdown step in the reaction process [6,27], by in situ DRIFTS measurements during the reaction before and after the shutdown step. Finally, we investigated the catalyst response to different procedures for a potential catalyst reactivation, which could at least partially offset the deactivation of the catalyst during reaction or shutdown, by following the evolution of the adlayer during reactivation (by DRIFTS) and evaluating changes in surface composition (by XPS). The reactivation procedures include thermal treatment in inert atmosphere (N_2) or treatment in oxidizing or reducing atmosphere.

2. Experimental

2.1. Catalyst preparation

The catalysts were prepared by a deposition-precipitation process, using commercial CeO_2 (HSA 15 from Rhodia, calcined in air at 400 °C) as support and $HAuCl_4{\cdot}4H_2O$ for deposition of Au. Further details have been given previously [28,29]. The Au metal content was determined by inductively coupled plasma atom emission spectroscopy (ICP-AES). All measurements were performed using catalysts with a BET surface area of 188 $m^2\,g^{-1}$ (2.8 wt% Au) or 78 $m^2\,g^{-1}$ (2.7 wt% Au). Before the reaction, the catalysts were activated by a reductive pretreatment at 200 °C (H200), which was previously shown to yield the most active catalysts [22].

2.2. Catalyst characterization

The chemical composition of the catalysts was characterized by XPS (PHI 5800 ESCA system), using monochromatized AlK_α radiation. The survey spectra were measured in the range of 0–1400 eV binding energy (BE), and detail spectra of the Au(4f) and Ce(3d) regions were measured in the ranges 75–100 eV and 875–925 eV (0.125-eV step width), respectively. To remove surface charging effects, the BEs were calibrated using the $Ce^{4+}(3d^{10}4f^{0}V^{n})$ (u''') signal at 916.6 eV as reference [21,30]. The fitting procedure was described earlier [21,22]. For XPS measurements, catalyst conditioning was performed ex situ in a tubular microreactor. The Au(4f) signal intensity was normalized relative to a constant Ce(3d) intensity.

The particle sizes and particle size distributions were determined by XRD and TEM. The XRD measurements were performed in a Siemens D5000 diffractometer using the CuK_α line. Au and ceria support particle sizes were calculated using Scherrer's equation. TEM measurements were carried out on a CM20 (Philips) electron microscope, operated at 200 kV (point-to-point resolution, 0.24 nm). The dispersion of the Au particles was calculated via the number-averaged mean particle size, evaluating typically several hundred particles typically evaluated.

2.3. Activity measurements

The activity measurements were performed in a quartz tube microreactor (4 mm i.d.) located in a ceramic tube oven with typically 75 mg of powder. To obtain differential conversions, the catalyst samples were partly diluted with α-Al_2O_3 (see Table 1), which is not active for the reaction in the studied temperature range (reaction temperature, 180 °C). Different reaction gas mixtures were investigated, including idealized reformate [1 kPa CO, balance N_2 (dry) + 2 kPa H_2O], H_2-rich idealized reformate [1 kPa CO, balance H_2 (dry) + 2 kPa H_2O], H_2-rich CO_2-containing idealized reformate [1 kPa CO, 1 kPa CO_2, balance H_2 (dry) + 2 kPa H_2O], and realistic reformate [4 kPa CO, 16.8 kPa CO_2, 1 kPa CH_4, balance H_2 (dry) + 20 kPa H_2O]. The gas flow was maintained at 60 Nml min^{-1}. Water was added to the gas stream using a saturation unit. The influent gas and effluent gas were analyzed by online gas chromatography (DANI, GC 86.10) with H_2 as the carrier gas. High-purity gases from Westphalen (CO 4.7, CO_2 5.0, N_2 6.0, H_2 5.0) were used. Evaluation of the Weisz criterion showed the absence of mass transport-related problems [31]. More details on the kinetic measurements have been given elsewhere [32].

2.4. Infrared measurements

In situ IR measurements were performed in a DRIFTS setup using a Magna 560 spectrometer (Nicolet), equipped with a MCT narrow band detector and a commercial in situ reaction cell unit (Harricks, HV-DR2). This setup allows measurements in a continuous flow of gas mixtures, equal to those used in the activity measurements, and at elevated temperatures. Typically, 400 scans (acquisition time, 3 min) at a nominal resolution of 8 cm^{-1} were co-added for one spectrum. The infrared data were evaluated as Kubelka–Munk units, which are linearly related to the adsorbate concentration [33]. To analyze the product gas flow, a gas chromatograph (Chrompack CP 9001) was connected to the exhaust of the DRIFTS cell. This setup has been described in more detail previously [34].

Table 1
Initial activity and deactivation of a Au/CeO_2 catalyst (2.8 wt% Au, BET surface area 188 $m^2\,g^{-1}$) for the WGS reaction in different reaction atmospheres (60 Nml min^{-1}, 180 °C)

Catalyst treatment	Initial activity (10^{-5} mol g^{-1} s^{-1})	Deactivation after 1000 min (%)	Increase in carbonate IR intensity (%)
Idealized reformate (1 kPa CO, balance N_2 (dry) + 2 kPa H_2O), catalyst dilution 1:20	81	26.3	43
H_2-rich idealized reformate (1 kPa CO, balance H_2 (dry) + 2 kPa H_2O), catalyst dilution 1:20	23	27.7	87
H_2-rich, CO_2-containing idealized reformate (1 kPa CO, 1 kPa CO_2, balance H_2 (dry) + 2 kPa H_2O), pure catalyst	2.3	37.5	142
Realistic reformate (4 kPa CO, 16.8 kPa CO_2, 1 kPa CH_4, balance H_2 (dry) + 20 kPa H_2O), pure catalyst	5.3	57.6	174

3. Results and discussion

3.1. Catalyst composition and particle sizes on reaction in different reaction atmospheres

Before evaluating the chemical composition and morphology of the catalysts, we characterized these with respect to activity, stability, and buildup of reaction side products. Kinetic measurements performed during the WGS reaction (Fig. 1S, supplementary information) led to similar results as reported previously [24], with the initial activity decreasing in the order idealized reformate > H_2-rich idealized reformate > realistic reformate > H_2-rich CO_2-containing idealized reformate, and the extent of deactivation over 1000 min decreasing in the order realistic reformate > H_2-rich CO_2-containing idealized reformate > H_2-rich idealized reformate ≈ idealized reformate (Table 1). DRIFTS measurements of the build-up of adsorbed side products performed during these runs also yielded similar results to those described previously [24], demonstrating the buildup of bidentate and bridged adsorbed formates and of monodentate and bidentate carbonates on the catalyst surface (Fig. 2S, supplementary information), with the respective amounts depending on the reaction conditions.

The chemical composition of the catalyst was characterized via the Au(4f) and Ce(3d) signals recorded after reductive conditioning and after 1000 min of reaction in the different reaction atmospheres. XP spectra of the Au(4f) and Ce(3d) peaks are shown in Figs. 1 and 2, respectively. The Au(4f) signals were fitted by a Au^0 peak at 84.0 eV and a Au^{3+} peak at 87.7 eV (see [21,22] and references therein); the contributions from the different Au states are summarized in Table 2. Using additional peaks in the fitting procedure (e.g., a peak at 84.6 eV [4]) would improve the fit slightly; however, due to the ongoing discussion on the origin of the latter state [35], this was not included, because of an ionic Au state in the fit. After reductive pretreatment at 200 °C (H200) (Fig. 1a), the Au(4f) spectrum showed a Au^{3+} content of about 20%. On reaction, the contribution from cationic gold decreased to 14.1%, 8.7%, and 7% Au^{3+} for reaction in idealized reformate, H_2-rich idealized reformate, and H_2-rich CO_2-containing idealized reformate, respectively. Thus, the loss of activity accompanied a decrease in Au^{3+} content. On the other hand, in the more oxidizing atmosphere of the realistic reformate (with 20 kPa H_2O), the decrease in Au^{3+} content (12.8%) was less pronounced than in the other cases, whereas the deactivation was stronger than in the other reaction atmospheres.

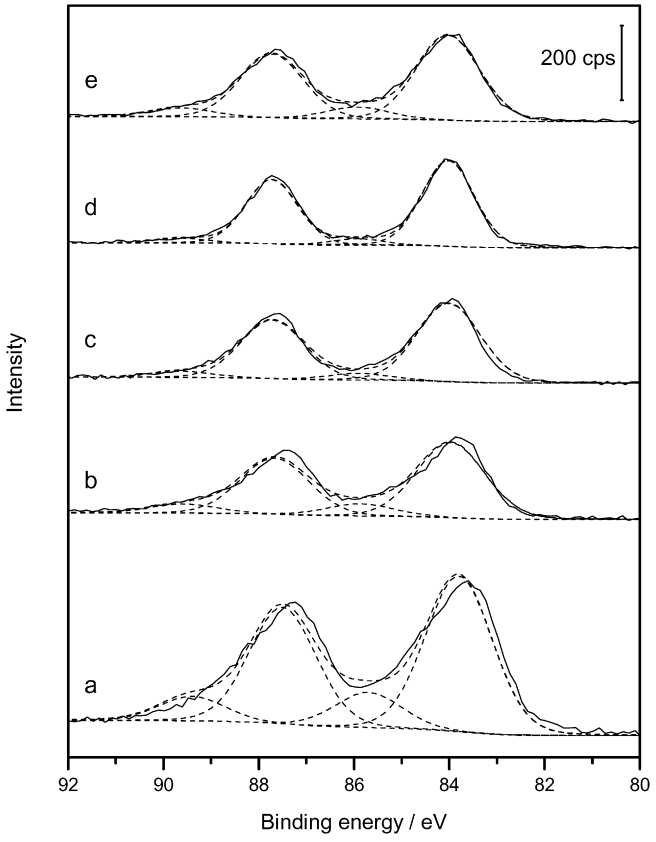

Fig. 1. XP spectra of the Au(4f) region of a 2.8 wt% Au/CeO_2 catalyst after (a) 10% H_2/N_2 at 200 °C, (b) idealized reformate (1 kPa CO, 2 kPa H_2O, rest N_2), (c) H_2-rich idealized reformate (1 kPa CO, 2 kPa H_2O, rest H_2), (d) H_2-rich CO_2-containing idealized reformate (1 kPa CO, 1 kPa CO_2, 2 kPa H_2O, rest H_2), and (e) realistic reformate (4 kPa CO, 16.8 kPa CO_2, 1 kPa CH_4, 20 kPa H_2O, rest H_2).

In addition, the relative Au(4f) intensity, normalized to a constant Ce(3d) intensity, changed during the reaction; however, the changes depended sensitively on the reaction atmosphere. Reaction in idealized reformate or in H_2-rich idealized reformate resulted in a decrease in the relative Au intensity by about half. For reaction in H_2-rich CO_2-containing idealized reformate, the decrease was less pronounced, and reaction in re-

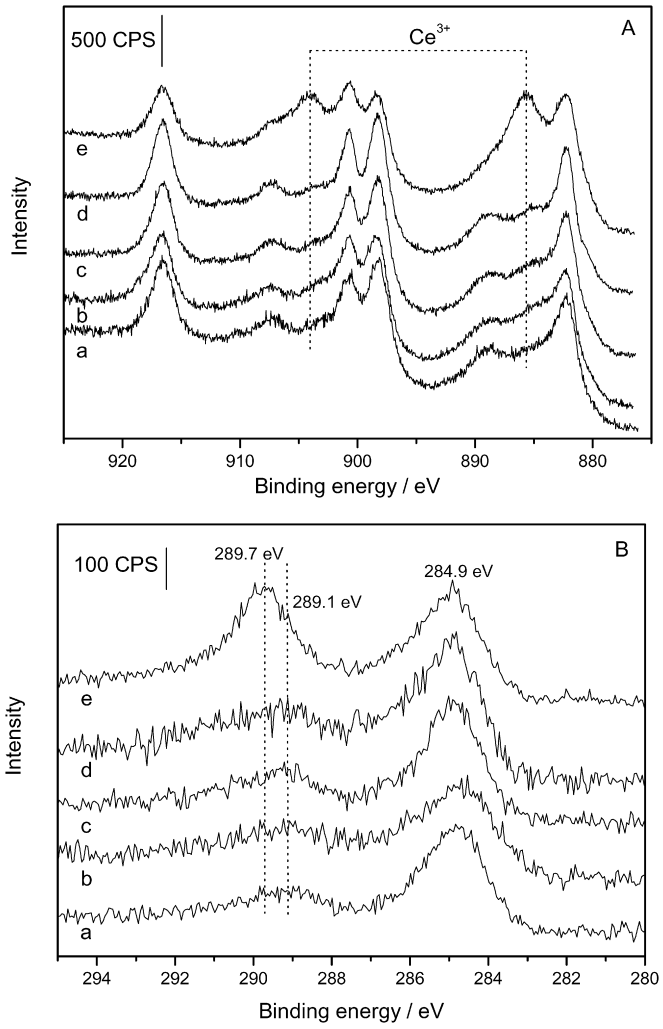

Fig. 2. XP spectra of the (A) Ce(3d) and (B) C(1s) regions of a 2.8 wt% Au/CeO_2 catalyst after (a) 10% H_2/N_2 at 200 °C, (b) idealized reformate (1 kPa CO, 2 kPa H_2O, rest N_2), (c) H_2-rich idealized reformate (1 kPa CO, 2 kPa H_2O, rest H_2), (d) H_2-rich CO_2-containing idealized reformate (1 kPa CO, 1 kPa CO_2, 2 kPa H_2O, rest H_2), and (e) realistic reformate (4 kPa CO, 16.8 kPa CO_2, 1 kPa CH_4, 20 kPa H_2O, rest H_2).

Table 2
Influence of the reaction gas mixture on the oxidation state of the Au/CeO_2 catalyst (BET surface area 188 $m^2\,g^{-1}$)

Catalyst treatment	Au^{n+} (%)	Ce^{3+} (%)	I_{Au}/I_{Ce} ratio
H200	19.7	20.9	0.096
Idealized reformate	14.1	26.7	0.049
H_2-rich idealized reformate	8.7	24.9	0.044
H_2-rich, CO_2-containing idealized reformate	7.0	23.6	0.039
Realistic reformate	12.8	44.0	0.048

alistic reformate even led to a small increase in the normalized Au(4f) intensity.

XPS spectra of the Ce(3d) region recorded after similar treatment are shown in Fig. 2 (upper panel). Applying the deconvolution procedure described previously [21,22,30], we determined a Ce^{3+} concentration of about 21% on the reductively pretreated catalyst, which agrees well with our previous findings [21,22]. After exposure to a 1000-min WGS reaction in idealized reformate, in H_2-rich reformate, and in H_2-rich CO_2-containing idealized reformate, this increased to about $25 \pm 1\%$ Ce^{3+} (Fig. 2; Table 2). For reaction in realistic reformate, the increase in Ce^{3+} content was much more pronounced, reaching about 44%, almost double that after reaction in H_2-rich idealized reformate. Apparently, realistic reformate, with its greater amounts of CO and H_2O, is more reductive for ceria by reaction of CO with surface oxygen, whereas Au^{n+} species are more easily reduced by H_2 in H_2-rich (CO_2 containing) idealized reformate. Furthermore, the C(1s) spectra (Fig. 2, lower panel) show peaks at 284.9, 289.1, and at 289.7 eV, which can be attributed to carbon contamination (284.9 eV) [36] and to surface carbonate and formate species (289.1 and 289.7 eV) [18,36–38].

Before discussing these results in more detail, we first present TEM and XRD data on the reaction-induced changes in the structural properties. Because of the low contrast between Au and Ce, Au particles are hardly detectable by TEM for similar sized Au and CeO_2 particles [22]. Thus, we used an Au/CeO_2 catalyst with a lower BET surface area (78 $m^2\,g^{-1}$) for the TEM evaluation of the reaction-induced modifications of the Au particle size. This catalyst contains similar-sized Au nanoparticles as the higher-surface area catalyst and exhibits comparable reaction characteristics after the same activation procedure (H200) [23]. The TEM images clearly demonstrate that the Au particles are homogeneously distributed on the catalyst before and after the WGS reaction; Fig. 3a gives a representative image. The particle size distributions obtained after reductive pretreatment and after WGS reaction in the different reaction atmospheres (Figs. 3b–3e) were rather broad, with a maximum at 2–2.5 nm (see Table 3). The resulting mean Au particle diameters scattered around 2.2 ± 0.7 nm. Including the XRD data (see below) also demonstrates that the slight increase in Au particle size during the reaction (from 2.0 ± 0.6 nm to about 2.2 ± 0.7 nm after the reaction, with small variations for the different reaction atmospheres) was at the limit of experimental significance.

Similar results were obtained from the X-ray diffractograms shown in Fig. 4 (see also Table 3). In general, the XRD-based particle sizes were slightly smaller than the TEM based values (by about 0.3 nm), but the trends are identical, with at most a slight increase during the WGS reaction but no resolvable effect of the different reaction atmospheres. The XRD measurements were performed on both the 78 and the 188 $m^2\,g^{-1}$ catalysts; in the latter case, no difference was found among the catalysts exposed to different reaction atmospheres during operation.

Comparison with previous studies and data leads to the following results. Fu et al. [1] reported a sintering of the Au particles from 4.6 nm (fresh catalyst, activation by calcination in air at 400 °C) to 6.8 nm for a Au/CeO_2 catalyst with 82.7 $m^2\,g^{-1}$ BET surface area (after WGS reaction in realistic reformate with 7% CO, 38% H_2O, 11% CO_2, 40% H_2, and He balance) based on XRD measurements. In this case, however, the reaction temperature (300 °C) was significantly higher than in the present measurements. Sintering was less strong during reaction in dilute water gas (2% CO, 10% H_2O in He, 300 °C),

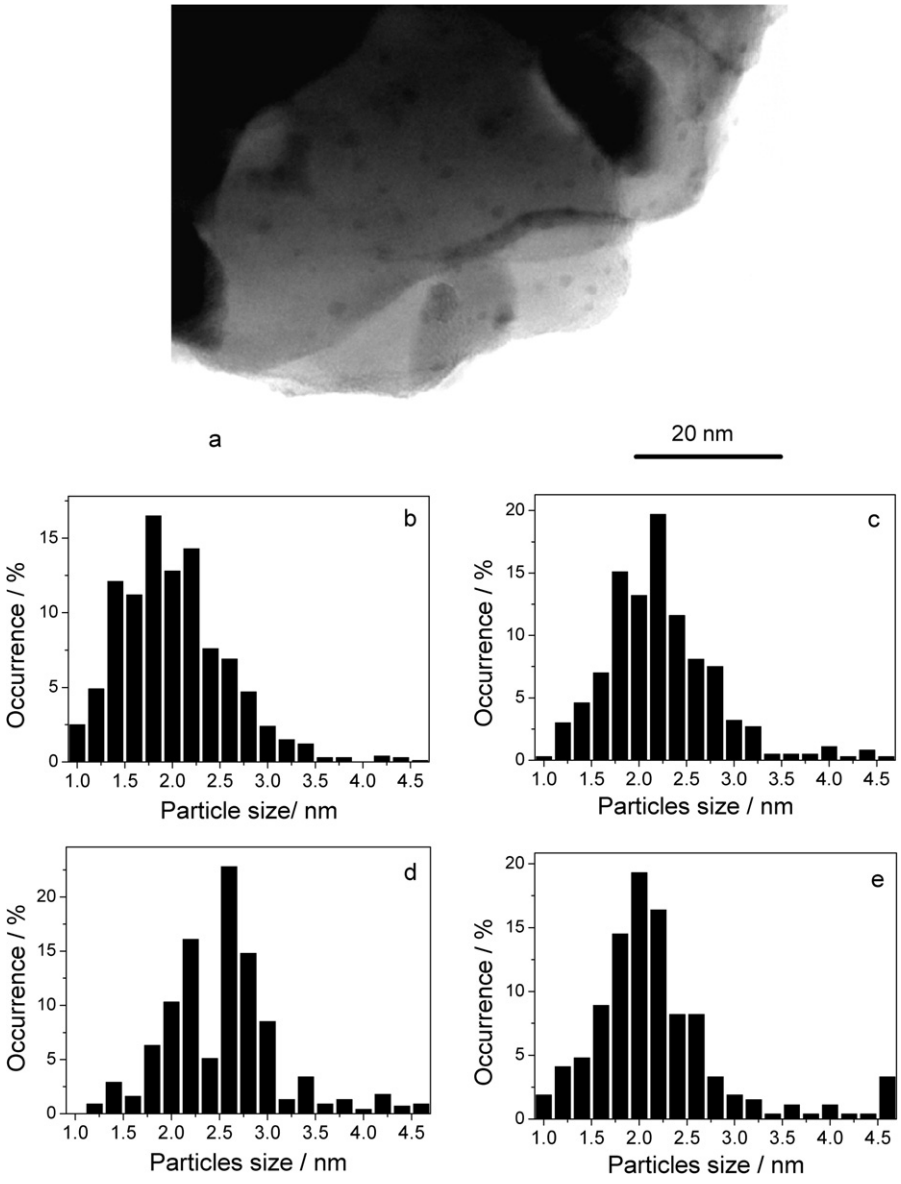

Fig. 3. (a) TEM image of the 2.7 wt% Au/CeO_2 catalysts (78 $m^2\,g^{-1}$) after 1000 min realistic reformate at 180 °C (H200) and particle size distribution of the (b) reductive treatment at 200 °C (H200), (c) idealized reformate (1 kPa CO, 2 kPa H_2O, rest N_2), (d) H_2-rich CO_2-containing idealized reformate (1 kPa CO, 1 kPa CO_2, 2 kPa H_2O, rest H_2), and (e) realistic reformate (4 kPa CO, 16.8 kPa CO_2, 1 kPa CH_4, 20 kPa H_2O, rest H_2).

Table 3
Au particles sizes as determined from TEM and XRD data

Catalyst treatment	TEM		XRD	
	Au particles[a]	d_{Au} (nm)[a]	d(Au(111)) (nm)[a]	d(Au(111)) (nm)[b]
H200	721	2.0 ± 0.6	1.7 ± 0.2	2.0 ± 0.2
Idealized reformate	372	2.2 ± 0.6	2.0 ± 0.2	1.8 ± 0.1
H_2-rich, CO_2-containing idealized reformate	447	2.5 ± 0.7	1.9 ± 0.1	1.8 ± 0.1
Realistic reformate	269	2.2 ± 0.8	1.8 ± 0.1	1.8 ± 0.1

[a] Au/CeO_2 catalyst with 78 $m^2\,g^{-1}$ surface area.
[b] Catalyst with 188 $m^2\,g^{-1}$ surface area.

where the Au particle size increased from 5 nm (fresh catalyst with 155.8 $m^2\,g^{-1}$ BET) to 6.2 nm. Later, the same authors proposed that Au^{n+} species represent the active sites of the Au/CeO_2 catalyst [4] and that growth of Au nanoparticles is not responsible for the deactivation [6]. Kim and Thompson arrived at a similar conclusion [18]. In contrast, Luengnaruemitchai et al. [9] reported significant Au particle growth, from 4 to 5.5 nm (by XRD and TEM), during deactivation of their Au/CeO_2 catalyst in idealized reformate (2% CO, 20% H_2O in He, reaction temperature 360 °C). A completely different behavior—a decrease in the size of Au particles during the WGS reaction in idealized reformate (4.5 kPa CO, 31.1 kPa H_2O, rest Ar, 200–260 °C) from 5.5 nm (3 wt% Au/CeO_2, before reaction) to 4.5 nm (after reaction) and essentially constant activity over 3 weeks of reaction—was reported by Andreeva [7], although the origin of the surprising stability was not discussed in detail. Finally, Barbier and Duprez proposed that deactivation of Me/CeO_2 (Me = Pt, Pd, Rh) catalysts is related to a decrease in the "specific perimeter" by a change in metal particle shape

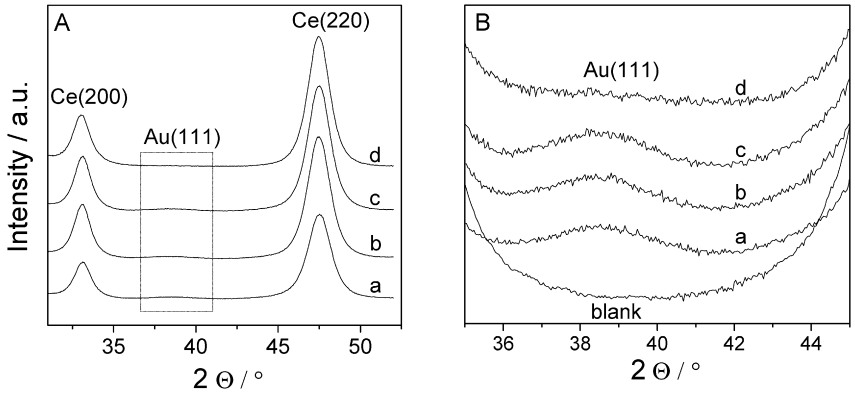

Fig. 4. XRD diffractograms of a 2.8 wt% Au/CeO_2 (188 $m^2\,g^{-1}$) catalyst after (a) reductive treatment at 200 °C (H200), (b) idealized reformate (1 kPa CO, 2 kPa H_2O, rest N_2), (c) H_2-rich CO_2-containing idealized reformate (1 kPa CO, 1 kPa CO_2, 2 kPa H_2O, rest H_2), and (d) realistic reformate (4 kPa CO, 16.8 kPa CO_2, 1 kPa CH_4, 20 kPa H_2O, rest H_2). (A) Complete XRD diffractogram and (B) enlarged part of the Au(111) and Au(200) lines.

Table 4
Ceria particle sizes as determined from XRD

Conditions	*d*(Ce(200)) (nm)[a]	*d*(Ce(220)) (nm)[a]	*d*(Ce(200)) (nm)[b]	*d*(Ce(220)) (nm)[b]
H200	13.4	10.8	7.2	5.3
Idealized reformate	13.4	10.9	7.2	5.4
H_2-rich, CO_2-containing idealized reformate	13.4	10.9	7.3	5.4
Realistic reformate	13.4	11.0	7.1	5.6

[a] Au/CeO_2 catalyst with 78 $m^2\,g^{-1}$ surface area.
[b] Catalyst with 188 $m^2\,g^{-1}$ surface area.

[39,40]. Changes in Au particle shape could occur together with the decrease in Au^{n+} content during the reaction—although, considering the small decrease in Au^{n+} content, we would expect such changes to be small. But, for the same reason as discussed earlier for the decreasing amount of Au^{n+} species, these changes in particle shape cannot represent the main cause of the Au/CeO_2 catalyst deactivation in our experiments.

We evaluated the possible growth of ceria particles during the WGS reaction, including the two different Au/CeO_2 catalysts with higher and lower BET surface areas (188 and 78 $m^2\,g^{-1}$, respectively), in the same way, comparing the mean particle sizes after reductive pretreatment at 200 °C and after 1000 min of reaction in idealized reformate, in H_2-rich CO_2-containing reformate, and in realistic reformate (Fig. 4; Table 4). For both Au/CeO_2 catalysts, we obtained stable line widths of the ceria (200) and (220) lines, indicating no sintering of the ceria particles during the WGS reaction in different reformates. Similar results were obtained by other groups for the stability of the ceria particles in Au/CeO_2 catalysts during the WGS reaction in different atmospheres (BET surface areas of 83–190 $m^2\,g^{-1}$) [1,5,6,18,41]. Bunluesin et al. [42,43] determined a measurable growth of the ceria particles during the WGS reaction at 300 °C for ceria (Pt, Pd, Rh)-supported catalysts and linked this to the strong catalyst deactivation; however, other effects could not be excluded from their measurements.

The XRD and TEM results clearly show that after reductive pretreatment at 200 °C, both the Au and ceria particle sizes remained essentially constant during 1000 min of WGS reaction at 180 °C. Therefore, irreversible particle sintering can be excluded as a significant contributor to the ongoing deactivation of the Au/CeO_2 catalyst under the present reaction conditions. The apparent discrepancy between our results on Au and ceria particle size and stability and previous data and proposals [6,9,41] for Me/CeO_2 catalysts (Me = Au, Pt, Pd) can be explained at least in part by the different reaction conditions; differences in the exact catalyst composition also may contribute.

Apparently, the significant decrease in relative Au(4f) intensity during the WGS reaction does not reflect a similarly pronounced increase in Au particle size. This decrease most likely results from a number of different effects, including possible variations in the Au particle shape, sintering of individual Au^{3+} ions incorporated into the CeO_2 surface to metallic Au nanoparticles, and decreased Ce(3d) intensity due to absorption by surface carbonate and formate species adsorbed on the ceria support.

Besides the clear correlation between catalyst deactivation and increase in monodentate surface carbonate concentration (see also [24]), we also found significant variations in the Au^{n+} and Ce^{3+} content. Independent of the reaction atmosphere, the Au^{n+} content decreased during the reaction, along with a generally slight increase in Ce^{3+} content. The quantitative correlation is less clear, however. For instance, the pronounced decrease in activity during reaction in realistic reformate is accompanied by a smaller decrease in Au^{n+} content compared with the other cases. Thus, the decay in Au^{n+} content cannot be considered a dominant cause of the drastically increased deactivation. On the other hand, the combination of higher reaction-induced increase in Ce^{3+} content and pronounced deactivation in this case does not fit the deactivation behavior in the other atmospheres, where the deactivation varied significantly with an increase in Ce^{3+} content that was small and of comparable extent.

In total, these different results do not support a general correlation between catalytic activity on the one hand and cationic Au^{n+} species or Ce^{3+} species/oxygen vacancies [44] as well as related changes in the Au particle shape [39,45] on the other hand—although the latter features may well affect the activity in combination with other effects, most prominently the monodentate carbonate coverage. We discuss this in more de-

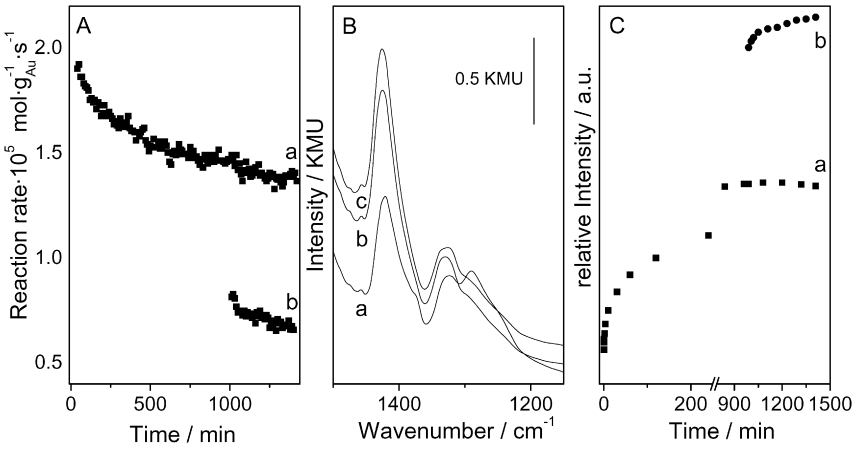

Fig. 5. Shutdown experiment: (A) activity kinetic measurement on a 2.8 wt% Au/CeO_2 (188 $m^2\,g^{-1}$) catalyst in H_2-rich CO_2-containing idealized reformate (1 kPa CO, 1 kPa CO_2, 2 kPa H_2O, rest H_2); (a, b) long-term WGS reaction without (a) and with shut-down (b) after 1000 min operation; (B) DRIFTS spectra (carbonate region) of the Au/CeO_2 catalyst after (a) 1000 min reaction, (b) after 60 min shut-down and re-heating in the reaction gas mixture to 180 °C, and (c) after 400 min additional WGS reaction; (C) relative intensity (to 1000 min) of the monodentate carbonate peak at 1421 cm^{-1} during long-time WGS reaction without (a) and with (b) with shut-down after 1000 min.

tail after presenting the reactivation data (Section 3.3). Finally, on a more general scale, the deactivation always will depend strongly on the reaction temperature, because higher reaction temperatures promote both carbonate decomposition (decreasing carbonate effects) and metal particle sintering (increased particle sintering effects).

3.2. Shutdown measurement

Shutdown experiments provide information on the response of the catalyst to the sudden change in reaction conditions on shutdown of the reaction. In the present case, we simulated this by cooling in reaction gas, equivalent to gas flow stoppage and reactor cool down in a technical setup. In previous experiments, such treatment led to considerable deactivation of the Au/CeO_2 catalysts in the subsequent reaction. Based on the evolution of CO_2 and H_2O in subsequent temperature-programmed oxidation (TPO) experiments, the deactivation was attributed to additional surface blocking by formation of adsorbed hydroxycarbonates [17]. A direct identification of these species as an origin of the decreasing activity remains elusive, however. Therefore, we investigated the changes in catalyst surface composition through activity measurements and in situ DRIFTS measurements under identical reaction conditions. In these experiments, the catalyst was operated in H_2-rich CO_2-containing idealized reformate for 1000 min, cooled to room temperature in the same gas flow, and, after 1 h in the reaction gas mixture, reheated to 180 °C and maintained for another 400 min in the same atmosphere. The catalyst activity decreased drastically (to about 43%) after the shutdown, and did not recover after the reheating step (Fig. 5Ab). DRIFTS measurements (Figs. 5B and 5C) show a strong increase of the monodentate carbonate peak at 1421 cm^{-1} after the shutdown, which remained stable after the subsequent reheating step. The close correlation between the carbonate peak intensity (Fig. 5C) and the decreasing activity (Fig. 5A) leads to the conclusion that in this case, this adsorbed monodentate carbonate species with a peak at 1421 cm^{-1} also acts as a deactivating byproduct that is largely responsible for the additional deactivation [21,24]. Under these conditions, Au or ceria particle sintering can be excluded, and ceria reduction should be less efficient, due to the low temperature. The lower deactivation reported by Fu et al. [6] for a similar shutdown/startup measurement on a (4.7 at% Au) Au/CeO_2 catalyst in realistic reformate (by 13%, compared with 57% in our measurements) can be convincingly explained by the higher reaction temperature (300 °C) in their measurements, which is high enough to facilitate partial carbonate decomposition on restarting the reaction.

In total, these results on the deactivation under shutdown conditions support our previous conclusions [24] that under the present reaction conditions (particularly at temperatures below 200 °C), adsorbed monodentate carbonate acts as a deactivating byproduct of the WGS reaction on Au/CeO_2 catalysts. Similar results (in situ DRIFTS) and conclusions also were derived for the WGS reaction on Pt/CeO_2 [27]. At these low reaction temperatures, the carbonate decomposition rate is too low to keep the steady-state carbonate coverage at sufficiently low levels. Therefore, the additional surface carbonate formed during shutdown cannot be removed again by restarting the reaction.

3.3. Au/CeO_2 catalyst regeneration

The response of the (partly) deactivated catalyst to a chemical or thermal treatment is interesting not only for practical reasons (e.g., for catalyst reactivation), but also for a mechanistic understanding of the deactivation process. Catalyst reactivation is possible only for a reversible deactivation (e.g., blocking of the catalyst surface or the active centers by solid side products such as carbonates [24,46] and/or reduction of the ceria substrate [25]), not for an irreversible deactivation (e.g., particle sintering). It was suggested earlier that the carbonate adlayer can be removed by reaction with O_2 or H_2O [24,46] or by heating in N_2 up to 500 °C [27]. Following these proposals, we investigated the effect of five different treatments on a 2.8 wt%

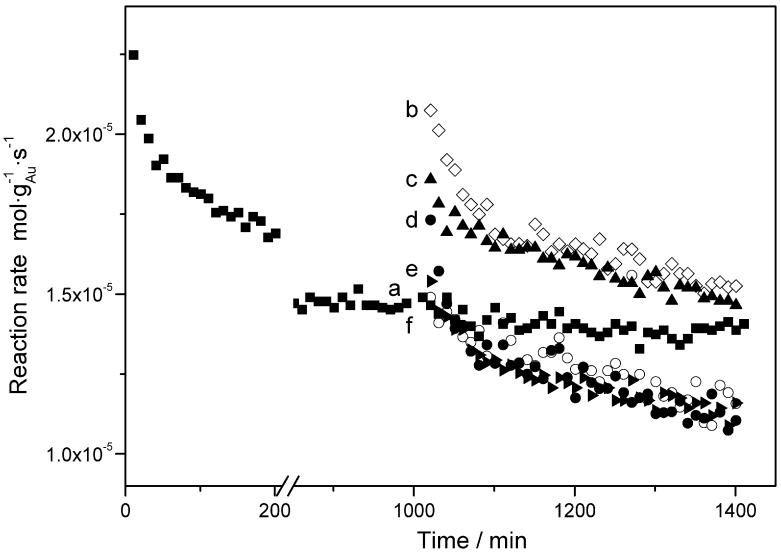

Fig. 6. Regeneration of the 2.8 wt% Au/CeO_2 catalysts after the WGS reaction in H_2-rich CO_2-containing idealized reformate (1 kPa CO, 1 kPa CO_2, 2 kPa H_2O, rest H_2) at 180 °C: (a) (■) long time WGS reaction without reactivation, (b–e) after reactivation (b) in 2 kPa H_2O/N_2 with subsequent H_2 reduction (◇), (c) in 2 kPa H_2O/N_2 (▲), (d) in 10% O_2/N_2 with subsequent H_2 reduction (●), (e) in 10% O_2/N_2 (►), and (f) in N_2 at 400 °C (○).

Au/CeO_2 catalyst (BET surface area, 188 $m^2\,g^{-1}$), which previously had been deactivated by 1000 min of reaction in a H_2-rich CO_2-containing idealized reformate. These treatments included exposure to H_2O- or O_2-containing gas mixtures (2 kPa H_2O, rest N_2, 4 h; 10 kPa O_2, rest N_2; 1 h; all 180 °C), with or without subsequent reduction in a H_2/N_2 mixture (10 kPa H_2, rest N_2, 30 min, 180 °C). Thermal reactivation was tested by heating to 400 °C in N_2 for 2 h. After reactivation, the catalyst was maintained for another 400 min in the initial reaction atmosphere. For comparison, we also included the behavior of the catalyst activity over 1400 min without additional treatment.

The results of the activity measurements, presented in Fig. 6, demonstrate that catalyst activity could be increased significantly by these treatments, and, in one case [oxidation in water vapor and subsequent reduction in H_2 (Fig. 6b)] initial activity could be regained almost completely. The second-highest activity was achieved by water treatment without subsequent reduction (Fig. 6c). In both cases, however, the reaction rate quickly decayed again during the subsequent WGS reaction, in about the same way as was observed for the freshly conditioned catalyst. After 400 min of reaction, the activity was close to that of the nonactivated catalyst. After O_2 treatment, regeneration was much less efficient (with subsequent reduction) or even absent (no subsequent reduction). The subsequent decay in activity proceeded to levels significantly below that of the nonactivated catalyst after 1400 min. Similar observations were made for thermal treatment (N_2, 400 °C). The generally rapid decay of the activity after regeneration clearly demonstrates that obtaining long-term improvement of catalyst performance, as would be desirable for technical applications, is not possible by these reactivation procedures.

DRIFTS measurements performed during and after the different chemical reactivation procedures described above are shown in Fig. 7. For reactivation in the O_2/N_2 mixture (Fig. 7, top left, a), the surface composition changed rapidly. After the first minute of the reactivation process, a negative band at 2126 cm^{-1} appeared in the CO-region, which is attributed to the removal of (surface) Ce^{3+} species ([23] and references therein). Apparently, the Ce^{3+} species are rapidly oxidized to Ce^{4+}. Furthermore, also the bidentate and bridged formate species decomposed during the first minutes. The monodentate carbonates were more stable under oxidative conditions, but also disappeared after about 10 min reaction. Subsequent reduction in 10 kPa H_2, rest N_2 did not affect the surface composition, except for regeneration of Ce^{3+} species. Hence, oxidation in O_2 at 180 °C resulted in complete decomposition of the adsorbed reaction side products, both with and without subsequent reduction. Deng and Flytzani-Stephanopoulos [17] reported a beneficial effect of O_2 on the deactivation of Au/CeO_2 catalyst from slower hydroxycarbonate formation for the WGS reaction as well as for shutdown/startup operation. Reactivation in a H_2O/N_2 gas mixture showed a similar general behavior (Fig. 7, top right) as in O_2/N_2 atmosphere, including the oxidation of Ce^{3+} species. The rate of Ce^{3+} oxidation was slower in water vapor than in the O_2/N_2 atmosphere. The use of water also diminished the amount of adsorbed surface species, but some especially most of the monodentate carbonates (characteristic peak at 1418 cm^{-1}), bridge-bonded formates (characteristic peaks at 2932 and 2960 cm^{-1}), and less reactive bidentate formate (characteristic peaks at 1560 and 2858 cm^{-1}), remained present on the ceria surface. In contrast to those species, bidentate formate was fully decomposed by contact with water, as discussed previously [21].

Changing back to the initial reaction atmosphere (Fig. 7, bottom left and bottom right), the same surface species, both reaction intermediates (bidentate formates [21]) and stable side products (monodentate carbonates) reappeared on the reactivated catalysts as was observed before the reactivation process. Most rapidly, the bidentate formates were formed and approached the steady-state level for formate formation and de-

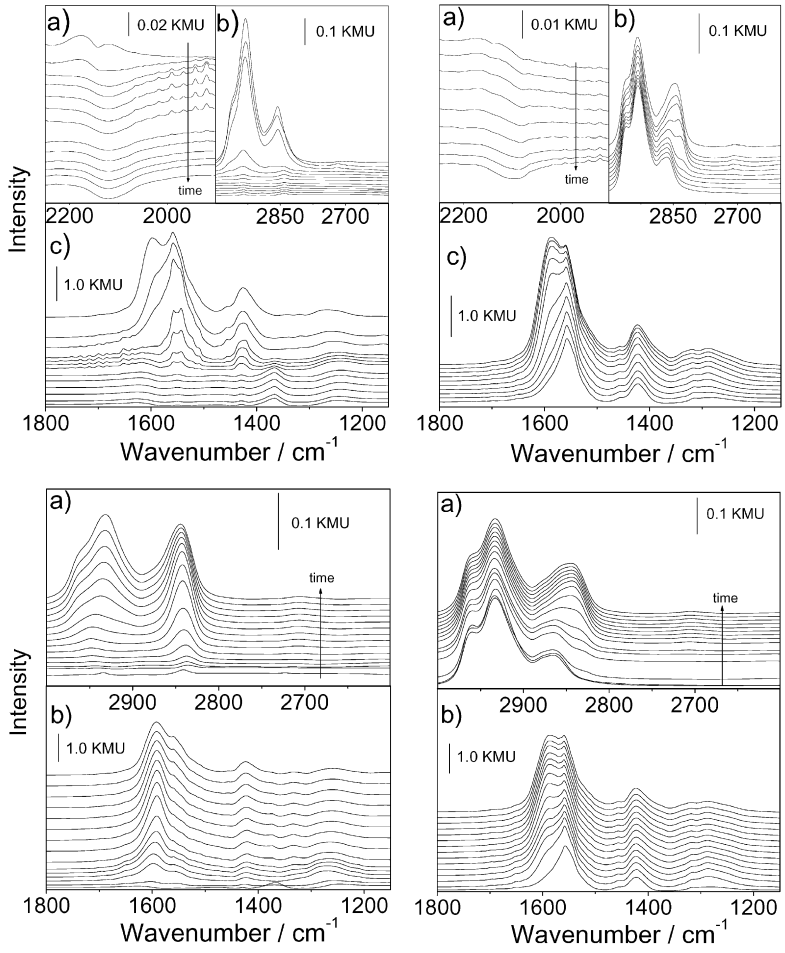

Fig. 7. DRIFT spectra of the regeneration of the 2.8 wt% Au/CeO_2 catalysts after the WGS reaction in H_2-rich CO_2 containing idealized reformate (1 kPa CO, 1 kPa CO_2, 2 kPa H_2O, rest H_2) at 180 °C. (Top left) regeneration in 10% O_2/N_2 (after 34 s, 71 s, 107 s, 178 s, 190 s, 202 s, 214 s, 335 s, 10 min, 15 min, 30 min, 60 min) and (bottom left) following 400 min reaction in H_2-rich CO_2-containing idealized reformate; (top right) in 2% H_2O/N_2 (after 34 s, 72 s, 132 s, 312 s, 10 min, 30 min, 60 min, 120 min, 180 min, 240 min) and (bottom right) following reaction (see above).

composition. In contrast, formation of the less active or reaction inhibiting other surface species (less reactive bidentate formate, bridge-bonded formate, monodentate carbonate) is slower. The relative time scales for the buildup of the respective adsorbed species are similar to those observed on freshly prepared catalysts after reductive conditioning [24]. Even after 400 min of reaction, the different abundance of surface species observed directly after reactivation in O_2/N_2 and after treatment in water vapor/N_2 was visible. In that case, the adlayer signals closely resembled those obtained after 1000 min of reaction without reactivation, whereas after O_2/N_2 treatment, the concentrations of these species were generally lower, and their relative amounts differed.

Changes in the oxidation state of the Au and ceria particle surfaces induced by the reactivation procedure were characterized by XPS measurements before and after that process (Fig. 8; Table 5). After reaction, the reactor was purged with N_2 to avoid reaction between CO (in the reaction gas) and O_2 (in the reactivation atmosphere). Reactivation by subsequent exposure to H_2O/N_2 or O_2/N_2 (with or without a subsequent reduction step) caused a further increase in Au^{3+} content from ∼7% to ∼28% (O_2 treatment) or ∼19% (oxidation in water vapor). The former value is even higher than that obtained after reductive pretreatment (H200, ∼20%). On the other hand, the reactivation treatments reduced the amount of Ce^{3+} to about 17% (O_2/N_2 treatment) or 20% (oxidation in H_2O/N_2), close to the value for a fresh catalyst after pretreatment in H_2/N_2 at 200 °C (21%). After the additional reduction step, the amount of Ce^{3+} increased to 22.4% (O_2/N_2 exposure) or 24.4% (H_2O/N_2 exposure). Thus, reactivation in O_2/N_2 at 180 °C led to the highest amount of Au^{3+} and the lowest amount of Ce^{3+}. The surface composition of the O_2/N_2-treated Au/CeO_2 catalysts came close to that of a fresh catalyst after oxidative pretreatment at 200 °C [22], whereas H_2O/N_2 reactivation, with or without an additional reduction step in H_2/N_2, resulted in a surface composition close to that obtained after reductive pretreatment. It was shown previously that reductive pretreatment yields higher activity than oxidative pretreatment (at the same temperature, 200 °C), which resembles the trend for reactivation in H_2O or O_2 [22].

The correlation between monodentate carbonate decomposition and reactivation of the catalyst supports our previous assignment of monodentate carbonates as a major cause of catalyst deactivation. The efficiency of the H_2O treatment for catalyst regeneration can be explained by a H_2O-induced desta-

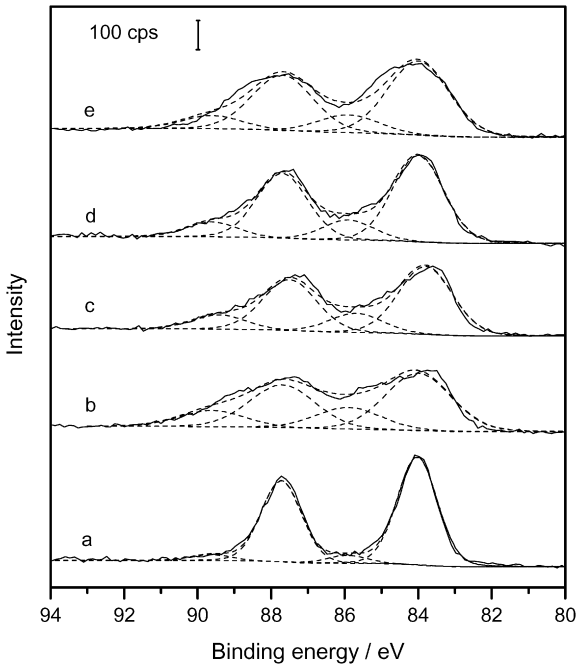

Fig. 8. XP spectra of the of the Au/CeO_2 catalysts (Au(4f) region) after (a) 1000 min WGS reaction in H_2-rich CO_2-containing idealized reformate (1 kPa CO, 1 kPa CO_2, 2 kPa H_2O, rest H_2) at 180 °C, and after subsequent reactivation in (b) 10% O_2/N_2, (c) 10% O_2/N_2 with following H_2 reduction, (d) 2 kPa H_2O/N_2 and (e) 2 kPa H_2O/N_2 with following H_2 reduction.

Table 5
Content of the Au^{n+} and Ce^{3+} after the WGS reaction and the different reactivation procedures as measured by XPS

Catalyst treatment	Au^{n+} (%)	Ce^{3+} (%)	I_{Au}/I_{Ce} ratio
After H200 pretreatment	19.7	20.9	0.096
After 1000 min WGS in H_2-rich, CO_2-containing idealized reformate	7.0	23.6	0.039
+ 60 min 10% O_2/N_2	27.8	17.3	0.042
+ 60 min 10% O_2/N_2 + 10% H_2/N_2	22.3	24.4	0.040
+ 240 min 2% H_2O/N_2	19.1	19.9	0.041
+ 240 min 2% H_2O/N_2 + 10% H_2/N_2	19.6	22.4	0.049

bilization of the monodentate carbonates, reaction to less stable bicarbonates, and subsequent thermal decomposition of the latter species [47,48]. For the same reason, deactivation is much lower for reaction in H_2O-rich gas mixtures with low CO or CO_2 content compared with that in atmospheres with low H_2O content [24]. Nevertheless, the lower activity obtained after O_2/N_2 reactivation (plus subsequent H_2 reduction) compared with the H_2O/N_2 treatment despite the more efficient carbonate removal in the former case clearly indicates that other effects also must be considered. The initially different activities of the reactivated catalysts directly after reactivation also may be related to the different relative amounts of Au^{n+} and Ce^{3+} species. But this can hardly explain the much lower activity of the catalysts reactivated by O_2/N_2 treatment or N_2 annealing after 400 min WGS reaction, where differences in the initial surface composition would be largely removed by reaction with the reaction gas mixture. Therefore, the differences in the final activity point to an additional contribution from an irreversible deactivation process. We propose that the lower activity after the O_2 treatment is at least partly related to O_2-induced sintering of the Au particles. The measured temperature in the microreactor (4 mm i.d., 75 mg Au/CeO_2 catalyst) indeed increased by 12 °C on switching to the O_2/N_2 mixture, and the increase in the catalyst bed at the catalyst surface may be significantly higher. The temperature increase can result from an exothermic oxidation of the catalyst and possibly adsorbed species (formates) as well (see Fig. 7, top left and top right). In this case, the increased activity due to surface carbonate decomposition is (partly) compensated for by irreversible deactivation due to Au particle sintering. It is likely that particle sintering is also caused by N_2 annealing, considering that these catalysts were activated by reduction at 200 °C—at much lower temperatures than the 400 °C annealing step. This explanation agrees well with findings of Liu et al. [27], who observed no regeneration of a deactivated catalyst on heating to temperatures up to 500 °C. These authors also reported that the ongoing reformation of carbonates (reversible deactivation) during subsequent WGS reaction lea to a decay in activity to levels significantly below the initial activity [27], similar to our observations.

The aforementioned finding of an irreversible deactivation on O_2/N_2 treatment is contrasted by results of two recent findings, where annealing in O_2 or air at 300–450 °C was reported to be most efficient for regenerating a metal/CeO_2 (metal = Au, Pt) catalyst [17,27]. The apparent discrepancy with the present results may be associated with the higher pretreatment temperature of the catalyst (500 °C) [27] or the higher gas flow of reactants (2–3.5 times higher than in the present study) [17], where heat transport from the catalyst is faster than in the present case. Both effects make subsequent sintering less probable, leaving only the counteracting reactivation by carbonate decomposition. Our tentative proposal of Au sintering as major contributor to the lower catalyst reactivation on annealing in O_2 is supported by TEM measurements of catalyst after reactivation in O_2, which yielded a mean Au particle diameter of about 2.7 ± 0.8 nm (Fig. 9). In particular, the amount of Au particles with diameter >3 nm increased by about a factor of 2 after O_2 annealing.

Finally, the concomitant decay of the relative Ce^{3+} content and the monodentate carbonate coverage, together with the enhanced decomposition of the monodentate carbonate in an O_2 atmosphere, provides a simple explanation for the driving force behind this process. Apparently, the monodentate carbonate species are stabilized by neighboring Ce^{3+} species, adjacent to the carbonate-carrying Ce ion, and oxidation of these species to Ce^{4+} destabilizes the carbonate, resulting in enhanced carbonate decomposition.

4. Conclusions

Investigating the deactivation of Au/CeO_2 catalyst during the low-temperature WGS reaction in different reaction atmospheres and the underlying physical origin by TEM, XRD, XPS, DRIFTS, and activity measurements, we showed that at reaction temperatures around 200 °C, the significant deactiva-

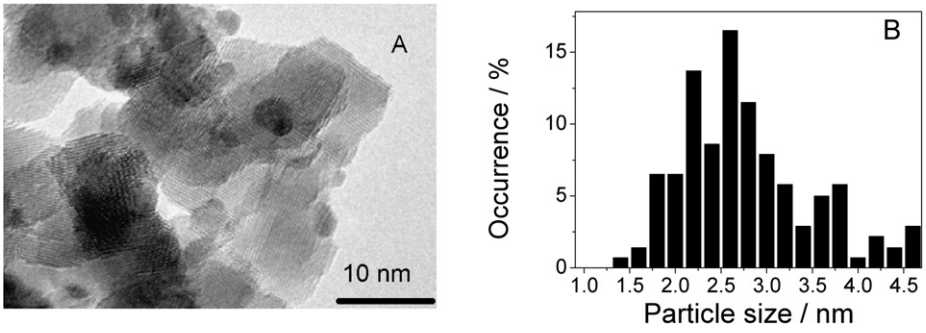

Fig. 9. TEM image (A) and particle size distribution (B) of the 2.7 wt%, 78 $m^2\ g^{-1}$ Au/CeO_2 catalyst after 1000 min WGS reaction in H_2-rich CO_2-containing idealized reformate (1 kPa CO, 1 kPa CO_2, 2 kPa H_2O, rest H_2) at 180 °C and subsequent reactivation in 10% O_2/N_2, showing an increasing content of larger particles compared to the catalyst without reactivation.

tion of Au/CeO_2-supported catalysts is related mainly to the formation of monodentate carbonates. These are adsorbed on the ceria support and possibly also on the active sites for formate formation and decomposition, and thus block the surface for the formation/decomposition of adsorbed formate species as reaction intermediates. Sintering of Au or ceria particles can be ruled out as a significant contributor to catalyst deactivation. Catalyst deactivation is also accompanied by a more or less pronounced decrease in Au^{n+} species and increase in Ce^{3+} species, depending on the reaction atmosphere. But the changes in catalyst surface composition are more complicated and cannot be interpreted in a simple manner, where, for instance, the decay in activity is quantitatively correlated with decreasing Au^{n+} content or increasing Ce^{3+} content. But at least the Ce^{3+} content appears to be correlated with the amount of adsorbed carbonate species, in the sense that carbonate formation can be reversed by Ce^{3+} oxidation, as demonstrated by the oxidative carbonate decomposition during reactivation. On the other hand, Ce^{3+} formation is not necessarily associated with carbonate formation, but can be caused by, for example, simple reduction by hydrogen in the reaction atmosphere. The less pronounced decay in the Au^{n+} content during reaction in realistic reformate compared with reaction in other atmospheres, together with the more pronounced deactivation in realistic reformate, clearly demonstrates that deactivation is not necessarily correlated with a decrease in Au^{n+} content, although a decrease in Au^{n+} content and possibly also related changes in the Au particle shape may contribute to the deactivation.

In summary, for reaction up to around 200 °C, catalyst deactivation is dominated by the formation of stable adsorbed monodentate carbonate species. Other effects, such catalyst reduction/oxidation, also may contribute but are less significant, confirming our previous proposal [24]. This conclusion is also supported by the results of in situ DRIFTS measurements of the deactivation during reaction shutdown and of similar measurements during different procedures for reactivation of a partly deactivated catalyst after 1000 min of reaction in H_2-rich CO_2-containing reformate, by reaction in O_2/N_2 or H_2O/N_2 mixtures with or without subsequent reduction in H_2/N_2, or by 400 °C annealing in inert atmosphere, and the subsequent WGS reaction on the reactivated catalyst. In the first case, activity and in situ DRIFTS measurements reveal that the significant deactivation during shutdown (by >50% relative to the activity before shutdown for reaction in H_2-rich CO_2 containing idealized reformate) is correlated with the additional buildup of monodentate carbonate species. In addition, for the reactivation experiments, the increase in activity on reactivation was coupled with a decrease in carbonate intensity (H_2O/N_2 treatment) or even complete removal of these species (O_2/N_2 treatment). In this case, however, other contributions can be identified as well. The lower activity after O_2/N_2 treatment compared with H_2O/N_2 reactivation, despite the complete removal of the carbonate species, can be explained by an additional contribution from irreversible deactivation due to Au particle growth.

Finally, the results demonstrate the need to investigate catalyst deactivation over a wide range of reaction parameters using various different techniques for the unambiguous identification of the different contributions to catalyst deactivation and their relative importance.

Acknowledgments

Financial support was provided by the Deutsche Forschungsgemeinschaft through Research Training Group 328 and project Be 1201/9-4, and by the Landesstiftung Baden-Württemberg.

Supplementary information

Supporting information for this article may be found on ScienceDirect, in the online version.

Please visit DOI: 10.1016/j.jcat.2007.05.016.

References

[1] Q. Fu, A. Weber, M. Flytzani-Stephanopoulos, Catal. Lett. 77 (2001) 87.
[2] R. Burch, Phys. Chem. Chem. Phys. 8 (2006) 5483.
[3] F. Meunier, D. Reid, A. Goguet, S. Shekhtman, C. Hardacre, R. Burch, W. Deng, M. Flytzani-Stephanopoulos, J. Catal. 247 (2007) 269.
[4] Q. Fu, H. Saltsburg, M. Flytzani-Stephanopoulos, Science 301 (2003) 935.
[5] Q. Fu, S. Kudriavtseva, H. Saltsburg, M. Flytzani-Stephanopoulos, Chem. Eng. J. 93 (2003) 41.
[6] Q. Fu, W. Deng, H. Saltsburg, M. Flytzani-Stephanopoulos, Appl. Catal. B 56 (2005) 57.
[7] D. Andreeva, Gold Bull. 35 (2002) 82.
[8] D. Andreeva, V. Idakiev, T. Tabakova, L. Ilieva, P. Falaras, A. Bourlinos, A. Travlos, Catal. Today 72 (2002) 51.

[9] A. Luengnaruemitchai, S. Osuwan, E. Gulari, Catal. Commun. 4 (2003) 215.
[10] T. Tabakova, F. Boccuzzi, M. Manzoli, D. Andreeva, Appl. Catal. A 252 (2003) 385.
[11] T. Tabakova, F. Boccuzzi, M. Manzoli, J.W. Sobczak, V. Idakiev, D. Andreeva, Appl. Catal. B 49 (2004) 73.
[12] T. Tabakova, F. Boccuzzi, M. Manzoli, J.W. Sobczak, V. Idakiev, D. Andreeva, Appl. Catal. A 298 (2006) 127.
[13] D. Tibiletti, A.A. Fonseca, R. Burch, Y. Chen, J.M. Fischer, A. Goguet, C. Hardacre, P. Hu, D. Thompsett, J. Phys. Chem. B 109 (2005) 22553.
[14] X. Wang, J.A. Rodriguez, J.C. Hanson, M. Perez, J. Evans, J. Chem. Phys. 123 (2005) 221101–221101-5.
[15] G. Jacobs, S. Ricote, P.M. Patterson, U.M. Graham, A. Dozier, S. Khalid, E. Rhodus, B.H. Davis, Appl. Catal. A 292 (2005) 229.
[16] W. Deng, J. De Jesus, H. Saltsburg, M. Flytzani-Stephanopoulos, Appl. Catal. A 291 (2005) 126.
[17] W. Deng, M. Flytzani-Stephanopoulos, Angew. Chem. 118 (2006) 2343.
[18] C.H. Kim, L.T. Thompson, J. Catal. 230 (2005) 66.
[19] C.H. Kim, L.T. Thompson, J. Catal. 244 (2006) 248.
[20] H. Sakurai, T. Akita, S. Tsubota, M. Kiuchi, M. Haruta, Appl. Catal. A 291 (2005) 179.
[21] R. Leppelt, B. Schumacher, V. Plzak, M. Kinne, R.J. Behm, J. Catal. 244 (2006) 137.
[22] A. Karpenko, Y. Denkwitz, V. Plzak, J. Cai, R. Leppelt, B. Schumacher, R.J. Behm, Catal. Lett., in press.
[23] A. Karpenko, R. Leppelt, V. Plzak, J. Cai, A. Chuvilin, B. Schumacher, U. Kaiser, R.J. Behm, Top. Catal. 44 (2007) 183.
[24] Y. Denkwitz, A. Karpenko, V. Plzak, R. Leppelt, B. Schumacher, R.J. Behm, J. Catal. 246 (2007) 74.
[25] J.M. Zalc, V. Sokolovskii, D.G. Loeffler, J. Catal. 206 (2002) 169.
[26] A. Goguet, F. Meunier, J.P. Breen, R. Burch, M.I. Petch, A. Faur Ghenciu, J. Catal. 226 (2004) 382.
[27] X. Liu, W. Reuttinger, X. Xu, R. Farrouto, Appl. Catal. B 56 (2005) 69.
[28] B. Schumacher, V. Plzak, M. Kinne, R.J. Behm, Catal. Lett. 89 (2003) 109.
[29] V. Plzak, J. Garche, R.J. Behm, Eur. Fuel Cell News 10 (2003) 16.
[30] M. Romeo, K. Bak, J. El Fallah, F. Le Normand, L. Hilaire, Surf. Interface Anal. 20 (1993) 508.
[31] P.B. Weisz, Chem. Eng. Prog. Symp. Ser. 55 (1992) 29.
[32] M.J. Kahlich, H.A. Gasteiger, R.J. Behm, J. Catal. 171 (1997) 93.
[33] I.M. Hamadeh, P.R. Griffiths, Appl. Spectrosc. 41 (1987) 682.
[34] M.M. Schubert, M.J. Kahlich, H.A. Gasteiger, R.J. Behm, J. Power Sources 84 (1999) 175.
[35] E.A. Willneff, S. Braun, D. Rosenthal, H. Bluhm, M. Hävecker, E. Kleimenov, A. Knop-Gericke, R. Schlögl, S.L.M. Schröder, J. Am. Chem. Soc. 128 (2006) 12052.
[36] J.F. Moulder, W.F. Stickle, P.E. Sobol, K.D. Bomben, in: Handbook of X-Ray Photoelectron Spectroscopy, Perkin Elmer Corp., Eden Prairie, 1992.
[37] D.R. Mullins, M.D. Robbins, J. Zhou, Surf. Sci. 600 (2006) 1547.
[38] O. Pozdnykova, D. Teschner, A. Wootsch, J. Kröhnert, B. Steinhauer, H. Sauer, L. Toth, F.C. Jentoft, A. Knop-Gericke, Z. Paál, R. Schlögl, J. Catal. 237 (2006) 17.
[39] J. Barbier, D. Duprez, Appl. Catal. B 3 (1993) 61.
[40] J. Barbier, D. Duprez, Appl. Catal. B 4 (1994) 105.
[41] X. Wang, R.J. Gorte, J.P. Wagner, J. Catal. 212 (2002) 225.
[42] T. Bunluesin, R.J. Gorte, G.W. Graham, Appl. Catal. B 14 (1997) 105.
[43] T. Bunluesin, R.J. Gorte, G.W. Graham, Appl. Catal. B 15 (1998) 107.
[44] J. Guzman, S. Carrettin, A. Corma, J. Am. Chem. Soc. 127 (2005) 3286.
[45] L. Barbier, B. Salanon, J. Sprösser, Surf. Rev. Lett. 88 (1994) 75.
[46] S. Hilaire, X. Wang, T. Luo, R.J. Gorte, J. Wagner, Appl. Catal. A 258 (2004) 271.
[47] B. Schumacher, Y. Denkwitz, V. Plzak, M. Kinne, R.J. Behm, J. Catal. 224 (2004) 449.
[48] R.J. Gorte, S. Zhao, Catal. Today 104 (2005) 18.